PHYSICAL REVIEW C VOLUME 57, NUMBER 6 JUNE 1998

Probing reaction dynamics with the ^{196}Pt$(n,xn\gamma)$ reactions for $x \leqslant 15$

L. A. Bernstein,[1] J. A. Becker,[1] W. Younes,[1] D. E. Archer,[1] K. Hauschild,[1] G. D. Johns,[2] R. O. Nelson,[2] W. S. Wilburn,[2] and D. M. Drake[3]

[1]*Lawrence Livermore National Laboratory, Livermore, California 94550*

[2]*Los Alamos National Laboratory, Los Alamos, New Mexico 87545*

[3]*Amparo Corporation, Santa Fe, New Mexico*

(Received 16 March 1998)

Discrete γ-ray spectra have been measured as a function of incident neutron energy for nuclei produced in the ^{196}Pt$(n,xn\gamma)$ reactions. Spectroscopy was done using the large-scale Compton suppressed Ge γ-ray spectrometer GEANIE. The ''white'' source neutron beam was produced at the Los Alamos Neutron Science WNR facility. Reaction neutron energy was determined using the time-of-flight technique. Reaction-channel yields were inferred from the measured intensity sum of the $2_1^+ \rightarrow 0_1^+$ and the $2_2^+ \rightarrow 0_1^+$ transitions for the ^{196}Pt(n,xn) reactions for $x \leqslant 15$. Weisskopf-Ewing calculations (including precompound) done with the HMS-ALICE code correctly predict the bulk of the (n,xn) reaction products for low multiplicity. However, they do not accurately predict yield ratios of the different (n,xn) reactions for $x \geqslant 9$. In addition, there is no consistent experimental indication of charged-particle reaction channels (n,pxn) for incident neutron energies above 60 MeV where they are predicted to account for approximately 1/3 of the total reaction cross section. Several possible causes are discussed for these discrepancies. Finally, the region of E-J phase space populated in this reaction is probed for several of the strongest reaction channels through the observation of relative yields for different yrast and off-yrast states. [S0556-2813(98)50706-6]

PACS number(s): 23.20.Lv, 24.10.−i, 25.40.Sc, 27.80.+w

Detailed information regarding high-excitation energy $[60 < E_x(\mathrm{MeV}) < 200]$, low-spin compound nuclear systems is sparse, in part due to the lack of high-energy light-ion accelerators coupled to large-scale γ-ray spectrometers. Several recent experiments using neutron beams fill in some of these gaps through the use of unusual combinations of reaction mechanisms and spectroscopic tools. Gill *et al.* [1] coupled the TESSA3 detector array to a reactor neutron source and added a plethora of information regarding off-yrast nuclear structure to the well-studied nucleus ^{168}Er. Vonach *et al.* [2] took advantage of the high-energy neutron beam at LANSCE/WNR to study the ^{208}Pb$(n,xn\gamma)$ reaction using γ-ray spectroscopy. They measured the $2_1^+ \rightarrow 0_1^+$ γ-ray yields for $x \leqslant 9$ using a combination of a single Ge detector and the WNR (Weapons Neutron Research) [3] spallation neutron source. Cross section results were presented in this experiment, and the effect of different level density formulations on the predicted cross section was tested. Only enough spectroscopy was performed to identify the reaction products, i.e., the decay of the first excited state in even-even products. We report here some first results from a new facility which couples the spectroscopic power of the large scale Compton suppressed Ge array, GEANIE (GErmanium Array for Neutron Induced Excitations), with the intense ''white'' neutron source at LANSCE/WNR. We measured yields of discrete γ rays produced in the ^{196}Pt(n,xn) reaction as a function of incident neutron energy for E_n between 3 and 250 MeV. These yields were used to determine which nuclei were formed and to probe the population of off-yrast and moderate spin states. Although we observed qualitative agreement between reaction theory and fractional reaction product yields for low-evaporated particle multiplicity, discrepancies were observed with model predictions for the higher evaporated particle multiplicity reactions $(x \geqslant 9)$, and for the charged particle channels throughout the incident neutron energy range.

GEANIE is a composite of the former HERA array from Lawrence Berkeley National Laboratory augmented by a suite of planar detectors. The array is comprised of a combination of Compton suppressed coaxial Ge detectors with approximately 25% of the efficiency of a 3 inch×3 inch NaI crystal and planar Ge detectors (LEPS, low energy photon spectrometers). GEANIE is located on the 60R flight path, 20.34 m from the WNR spallation neutron source, at the Los Alamos Neutron Scattering Center (LANSCE). Neutron energies at the WNR ''white'' source cover the range from less than 1 MeV to $\approx$ 600 MeV. The neutron flux falls rapidly between 5 and 20 MeV. The combination of the neutron flux, array efficiency and beam time allocation does not take advantage of the resolving power of the array for γ-γ spectroscopy in this experiment. We report results for a short run (44 hours) with sufficient statistics to allow for analysis of γ-ray singles up to incident neutron energies on the order of 250 MeV.

Reaction γ-rays produced by neutrons incident on a 97.4% isotopically enriched ^{196}Pt sample were measured with the following experimental setup: The target, two 0.54 gm/cm^2 foils, was placed at the focal point of GEANIE. The results presented in the current work were obtained with a partial implementation of GEANIE, consisting of 8 coaxial and 5 planar detectors (all suppressed). Spallation neutrons were produced at the W^{nat} spallation source driven by an 800 MeV proton beam with an average current of ≈ 2 μamp, and the following time structure: 100 Hz of ''macropulses,'' 625 μs long, composed of approximately 340 ''micropulses,'' spaced every 1.8 μs. The overall duty cycle was 6%. Recorded data consisted of γ-ray pulse heights corresponding

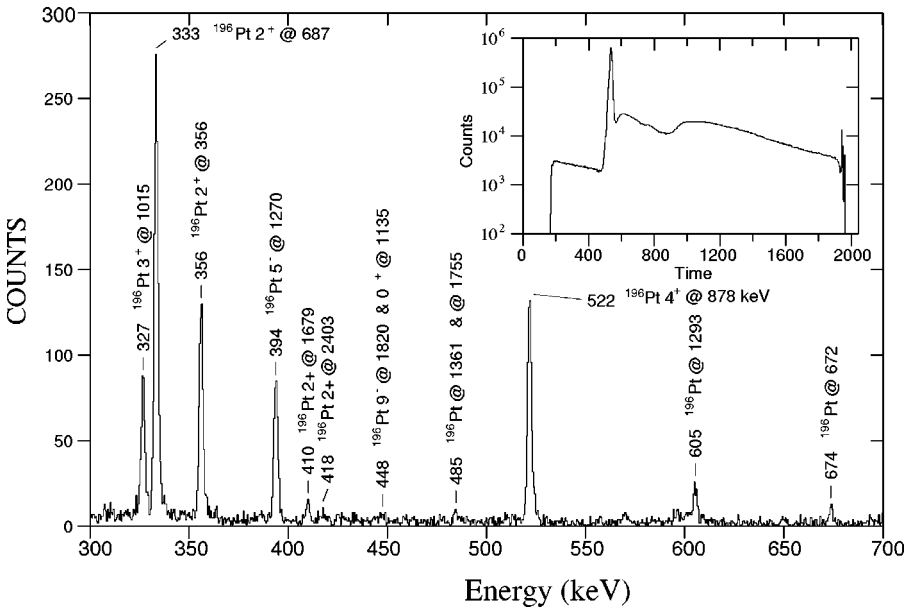

FIG. 1. Coincident gamma-ray spectrum (coaxial detectors) gated on neutron energy (1–8 MeV) and γ-ray energy (all members of the ground-state band up to $J=8\hbar$). Transitions in ^{196}Pt are marked by the J^{π} and E_x in keV of the parent level. The inset shows the time-of-flight spectrum for the planar detectors where the x axis has units of 4 ns (the TDC timing resolution) and the y-axis has units of counts.

to energies between 40 keV and 4 MeV together with the event time, correlated with respect to the beam micropulse RF signal. The time-of-flight method was used to obtain the energy of the reaction neutron. Data were taken for 44 hours and recorded onto magnetic tape. A total of 31 million γ singles and higher fold data were recorded (19 million coaxial and 12 million planar). Data acquisition was done using a specially modified version of the VME-based Michigan State University data acquisition system [4].

Although both γ-γ coincident and γ-singles data were recorded the small amount of coincident data ($\approx$2.1% of the total) precluded any significant additions to the already known Pt level schemes [5]. Nevertheless, the γ-ray spectrum shown in Fig. 1 from the coaxial detectors gated on neutron energy ($E_n=1-8$ MeV) and (in turn) the four lowest members of the ground state band illustrate the low background of the coincident data. Longer runs are likely to produce impressive results. Transitions are identified in Fig. 1 that indicate population of the known yrast and off-yrast states in ^{196}Pt with $J\leqslant 12\,\hbar$. The coincident data were also used to obtain the time resolution of the detectors from the FWHM of the prompt peak γ-γ timing spectra of all of the detector pairs. The average values for the coaxial (planar) detectors were FWHM$=34.4\pm0.3$ (14.1 ± 0.2) ns respectively.

The γ-ray singles data were analyzed over a wide range $[5\leqslant E_n(\mathrm{MeV})\leqslant 250]$ of incident neutron energy. Coincident data were unfolded, added to the singles data and sorted off-line into two γ-ray energy vs neutron time-of-flight matrices, corresponding to the two different detector types (coaxial and planar). The detector pulse heights and neutron time-of-flight for each detector channel of GEANIE were aligned in order to facilitate analysis of the data. The inset in Fig. 1 shows the total projections onto the time axis from the planar matrix (with time increasing from the left to the right). The largest peak in these spectra corresponds to the ''γ flash,'' produced when the incident proton beam strikes the spallation target. Counts to the right of the ''γ flash'' correspond to beam-correlated γ rays plus a time-independent background from target radioactivity. Counts to the left correspond mainly to target activity which is not temporally correlated with the immediately prior beam pulses; these counts were scaled and subtracted from the right-hand-side data to obtain the beam-induced spectrum. In addition to the background γ rays, the left-hand side of the spectrum includes ''wrap around'' events induced by low energy neutrons with time-of-flight longer than the time between micropulses (1.8 μs). The highest ''wrap-around'' neutron energy with the present experimental conditions is 650 keV. The only state in ^{196}Pt with an excitation energy below this is the yrast $J^{\pi}=2^+$ state at 356 keV. Therefore, this is the only state that can be populated by ''wrap-around'' neutrons. Contamination from the ''γ flash'' limited analysis to events with $E_n\leqslant 150(250)$ MeV for the coaxial (planar) detectors, respectively. Although there were nearly twice as many coaxial as planar detectors, the superior timing resolution of the planars made them far more useful for the observation of reaction products resulting from high energy $(E_n\geqslant 70$ MeV) neutrons.

Reaction products were identified on the basis of characteristic γ rays in spectra generated by making contiguous gates on the TOF axis of the E_γ-TOF matrices. The width of these gates corresponded to 5 MeV at low neutron energy and increased with greater neutron energy so as to match the uncertainty in energy determined by the detector timing of $\Delta E_n=1\sigma$. A particular reaction product was assigned if (a) at least three prompt transitions in the ground-state band were observed, and (b) the correct threshold behavior as a function of neutron energy was observed for each transition. Figure 2 shows a TOF-gated background subtracted planar spectrum with neutron energy gates between 120 and 220 MeV. All (n,xn) reaction channels with x odd up to $x=15$ were identified in the planar detector spectra set, whereas only $x=13$ were observed in the coaxial detectors spectra set. The limitation was due to contamination from the ''γ flash'' and an inability to align the timing signals due to their greater relative width.

Assignment of the odd-A and odd-odd reaction product γ rays was more difficult than for the even-even products due

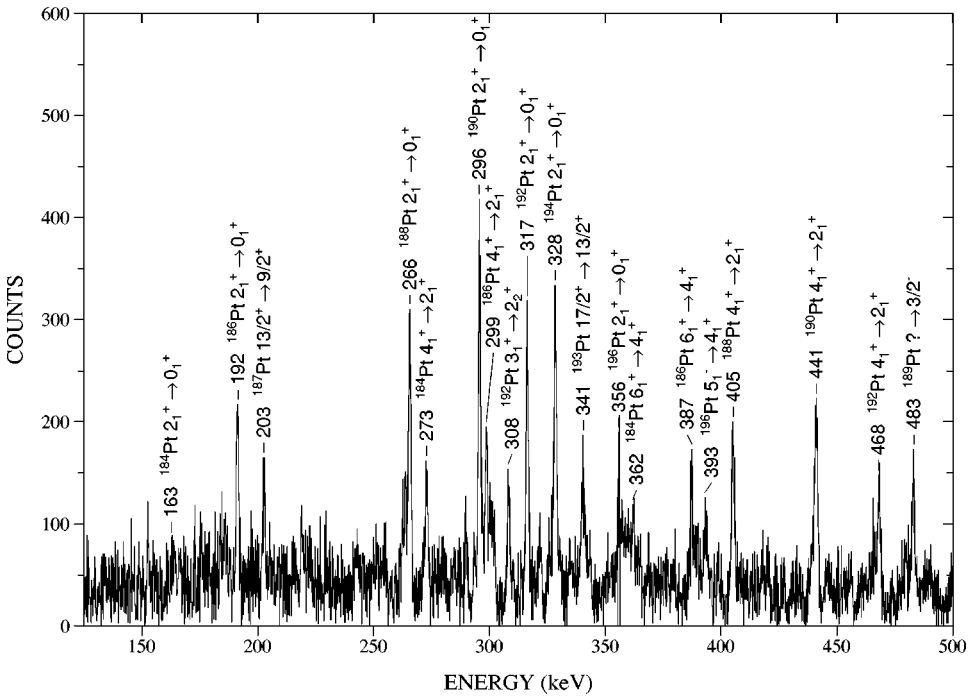

FIG. 2. Time-of-flight gated planar spectrum with $120 \leqslant E_n$ (MeV)$\leqslant 220$. Transitions in various (n,xn) reaction products are marked.

to greater fragmentation of the γ-ray strength caused by the higher level density at low excitation energy in these nuclei. Transitions were assigned to odd-mass Pt nuclei for all (n,xn) reactions with $x \leqslant 10$, but exhaustive searches failed to consistently place any set of transitions from an evaporation residue corresponding to a charged particle channel. The non-observation of the odd-odd Ir ($Z=77$) nuclei can be attributed to decreased individual γ-ray strengths due to fragmentation as well as the presence of isomeric states which would distort the measured time-of-flight. However, the lack of transitions in odd-mass Ir nuclei is more puzzling since the naive expectation would be that the γ-ray fragmentation in these nuclei should be comparable to that seen in the odd-A Pt. Recent results from a similar experiment studying neutron-induced reactions on a $^{\text{nat}}$Lu ($Z=71$) target using GEANIE suggest sizable discrepancies between experiment and the predictions of HMS-ALICE [6], highlighting the need for further examination of charged-particle reaction yields.

Absolute γ-ray partial cross sections require neutron flux and detector efficiency measurements which were not taken in this experiment. Thus it is not possible to make direct comparison of cross sections predicted by HMS-ALICE with measured γ-ray intensities. However, a surrogate is available. The $2_1^+ \rightarrow 0_1^+$ yield in even-even residues represents about 90% of the total reaction cross section [2], and this estimate can be improved by adding in the $2_2^+ \rightarrow 0_1^+$ yields. The detector efficiency-corrected intensity of the $2_1^+ \rightarrow 0_1^+$ and $2_2^+ \rightarrow 0_1^+$ transitions for each of the even-even Pt residues was extracted from the E_γ-TOF matrices, and summed. [The $2_2^+ \rightarrow 0_1^+$ feeding for all of the even-even Pt nuclei studied never exceeded 10% of the $2_1^+ \rightarrow 0_1^+$ intensity for all of the (n,xn) reaction channels.] The ratio of the yield for each of the even-even Pt residues over the total yield for all of the even-even products was then determined for every neutron energy. This ''fractional yield'' for a given reaction product, ^{x}Pt is given by the following expression:

$$Y_{\text{frac}}(^x\text{Pt}) = \frac{I_\gamma(^x\text{Pt}; 2_1^+ \rightarrow 0_1^+) + I_\gamma(^x\text{Pt}; 2_2^+ \rightarrow 0_1^+)}{\Sigma_{x=184}^{194} I_\gamma(^x\text{Pt}; 2_1^+ \rightarrow 0_1^+) + I_\gamma(^x\text{Pt}; 2_2^+ \rightarrow 0_1^+)}$$
$$x = \text{even}. \qquad (1)$$

The fractional yield is independent of the neutron flux for a given incident neutron energy range if the bin is kept small enough so that the flux does not vary across it appreciably. The measured fractional yield for each of the even-even Pt nuclei with $184 \leqslant A \leqslant 194$ is shown by the (♦) data points in Figs. 3(a)–3(f) over the energy range 10–200 MeV. The threshold for the (n,xn) reaction based on the known and calculated masses [7] for each of the reactions is indicated by the arrow on the x axis. The ^{196}Pt$(n,n')^{196}$Pt reaction is not included in this comparison due to contamination of the $2_1^+ \rightarrow 0_1^+$ transition by low-energy ''wrap-around'' neutrons. The ^{196}Pt$(n,15n)^{182}$Pt reaction is not included since the $2_2^+ \rightarrow 0_1^+$ transition was not identified.

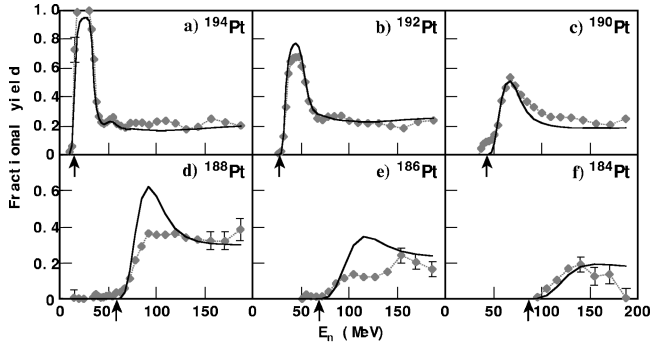

FIG. 3. Fractional yield plots from planar detectors (♦) and HMS-ALICE calculations (−) for even-mass Pt reaction products with $184 \leqslant A \leqslant 194$ (a–f). The HMS-ALICE calculations were weighted to reflect the detector timing. The arrows indicate the neutron energy threshold for formation of the reaction product based on the masses [7].

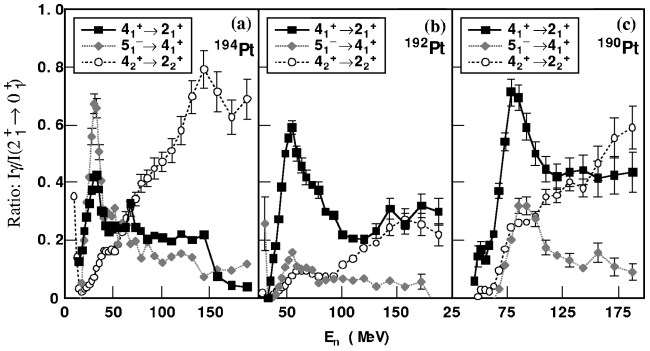

FIG. 4. γ-ray intensities as a function of incident neutron energy normalized to the yrast $2_1^+ \rightarrow 0_1^+$ transition for ^{194}Pt (a), ^{192}Pt (b), and ^{190}Pt (c) from the planar detectors for two yrast: $4_1^+ \rightarrow 2_1^+$ (■), $5_1^- \rightarrow 4_1^+$ (◆), and one off-yrast $4_2^+ \rightarrow 2_2^+$ (○) line.

The behavior of three structurally similar transitions was tracked over the same neutron energy range for the three (n,xn) reaction channels with $x=3$, 5, and 7. Contamination from stronger transitions in other channels made it difficult to track these transitions in the lighter Pt nuclei. The purpose of this analysis was to gain insight into which regions of energy-angular momentum (E-J) phase space were being populated at different values of incident neutron energy. The transitions tracked included the $4_1^+ \rightarrow 2_1^+$, the $4_2^+ \rightarrow 2_2^+$, and the $5_1^- \rightarrow 4_1^+$. The ratios of the yields for these transitions over the $2_1^+ \rightarrow 0_1^+$ transition as a function of neutron energy are presented in Figs. 4(a)–4(c).

We now compare measured gamma-ray yields with predictions of the HMS-ALICE code [8]. The nuclear model embodied in HMS-ALICE includes the Weisskopf-Ewing model of nuclear reactions (evaporation), together with a Monte Carlo treatment of precompound reaction mechanisms. The calculations were performed using the ''standard'' set of input parameters. These include a Fermi gas level density (for both nucleon and fission barrier states) with $a=A_{CN}/9$ and the A. J. Sierk fission barriers.

The comparison between experiment and the predictions of HMS-ALICE requires that the mapping of time-of-flight to incident neutron energy include the effect of the time dispersion of the Ge detector timing signal. The correction is nonlinear ($t \propto v^2$ for $E_n \ll m_n c^2$), and also depends on the γ-ray energy and the shape of the neutron flux. A time-of-flight gate corresponding to a nominal range of neutron energies has a neutron energy spread due to these effects that becomes greater at higher incident neutron energies where the time-of-flight becomes smaller (while the time dispersion remains constant). The predictions of a reaction code for discrete incident neutron energies over the entire range of neutrons energies from threshold to 190 MeV was weighted by a Gaussian distribution centered on the experimental centroid of the neutron energy bin with σ determined by the γ-γ timing resolution. The time-of-flight bins were kept small enough to insure that the neutron flux could be approximated as constant across them. These ''weighted'' calculations are shown for the timing resolution of the planar detectors by the solid lines in Figs. 3(a)–3(f).

Comparison of the model prediction and experimental results shows that HMS-ALICE qualitatively succeeds in reproducing the persistence of specific reactions at energies far above the reaction threshold. However, significant deviations between experiment and the calculations are evident for the $(n,xn\gamma)$ reaction with $x \geqslant 9$. It should be noted that although these deviations appear sizable in the graphs of fractional yield, they represent a small percentage of the summed (n,xn) cross section at higher neutron energies. Two possible explanations for these deviations follow. The first is that competition from other reaction channels resulting in odd-A Pt and Ir nuclei are not accurately predicted by the model calculations. This explanation is supported by the lack of observation of any strong, charged particle channels in the data. Another possible cause is that the relative strength of the compound nuclear and precompound reaction mechanisms are not correctly represented in the model. The differences in the shape of the curves for the theoretical and experimental fractional yield support this latter interpretation. A normalized cross section curve would provide a better comparison between experiment and theory than the fractional yields. This would aid in a determination of which of the two mechanisms described above is responsible for the deviations between experiment and theory. However, the lack of a neutron flux and an absolute detector efficiency measurement precludes this analysis of the current data.

The data from this experiment can also be used to gauge the relative population of nuclear states with different excitation energy and angular momentum as a function of incident neutron energy. We have restricted our study to a representative sample in the strongest reaction channels: $(n,3n\gamma)$, $(n,5n\gamma)$, and $(n,7n\gamma)$. The plots in Figs. 4(a)–4(c) give an appreciation for the variation in the population of two higher spin yrast states ($J^\pi=4^+$ and $J^\pi=5^-$) with increasing incident neutron energy. The plots show that these states are populated more strongly for neutron energies near threshold, where the compound nuclear reaction mechanism predominates. In contrast, the off-yrast $4_2^+ \rightarrow 2_2^+$ transition shown in Figs. 4(a)–4(c) is more intense with increasing incident neutron energy, where precompound mechanisms play a greater role. These results can be understood in terms of angular momentum conservation and the two competing reaction mechanisms involved. In a compound nuclear reaction the entire energy and angular momentum of the incident neutron is absorbed in the target nucleus and its energy equally distributed between all of the nucleons. The particles evaporated from this compound system for reactions with particle multiplicities greater than 1 have relatively low energy and are emitted isotropically, resulting in little or no loss of angular momentum and a relatively strong population of higher spin states. In contrast, the particles emitted following a precompound or ''knockout'' reaction mechanism have a sizable portion of the angular momentum of the incident neutron, resulting in a comparably smaller amount of residual angular momentum in the reaction product and a relatively greater population of off-yrast states. The shapes of these curves confirm that a transition occurs between these two reaction mechanisms as the incident neutron energy increases.

The combination of the GEANIE γ-ray spectrometer and the LANSCE/WNR high energy spallation neutron source offers a unique combination of high-resolution coincident and singles γ-ray spectroscopy of neutron-induced reaction products. Reaction mechanisms have been studied using the

^{196}Pt$(n,xn\gamma)$ reactions in the incident neutron energy range from $\approx$1 to over 200 MeV. All even-A Pt nuclei with $182 \leqslant A \leqslant 196$ and odd-A Pt nuclei with $195 \leqslant A \leqslant 187$ have been identified. A comparison of the fractional yields of the even-even Pt reaction products with the predictions of the HMS-ALICE model shows qualitative agreement for the reactions with lower evaporated nucleon multiplicity ($x \leqslant 7$) and significant deviations above this value. In addition, there appears to be a significant over-prediction of the charged particle channels. These differences might be attributable to experimental factors in the odd-A and odd-odd reaction products, including lessened γ-ray sensitivity due to fragmentation and/or isomeric states. However, inadequacies in the model calculations cannot be ruled out, including an inaccurate treatment of precompound reaction mechanisms and increased competition from reaction channels that result in odd-A products. Further experimental work is warranted, including a detailed neutron fluence and detector efficiency measurement, on targets with both even and odd numbers of protons and neutrons. Finally, calculations with codes that predict partial γ-ray cross sections to allow for a quantitative comparison between experiment and theory for channels that result in odd-A reaction products would be welcome.

A final note: observation of exotic reactions such as $(n,15n)$ in a run of such short duration with a partial implementation of GEANIE opens the possibility of using similar high-evaporated neutron multiplicity reactions to probe the low-lying off-yrast structure of exotic neutron-deficient nuclei, including most notably nuclei with $40 \leqslant N = Z \leqslant 50$. For example, (n, xn) reactions on the lightest stable Sn isotope, ^{112}Sn, result in the formation of very neutron-deficient Sn isotopes. Although charged particle evaporation is expected to play a larger role with decreasing proton number, recent results from the GEANIE detector using an ^{170}Er target [9] suggest that neutron emission will compete favorably with charged particle emission at high multiplicity of particle emission. Further experiments using neutron-deficient targets are necessary to determine how well $(n,xn\gamma)$ can be used to probe nuclei near the proton drip-line.

The authors would like to thank Mark Chadwick from Los Alamos for reading this manuscript and offering invaluable insight into reaction modeling. This was been made possible through the U.S. Department of Energy Contract numbers W-7405-ENG-48 (LLNL) and W-4705-ENG-36 (LANL).

[1] R. L. Gill *et al.*, Phys. Rev. C **54**, 2276 (1996).
[2] H. Vonach *et al.*, Phys. Rev. C **50**, 1952 (1994).
[3] P. W. Lisowski, C. D. Bowman, G. J. Russell, and S. A. Wender, Nucl. Sci. Eng. **106**, 208 (1990).
[4] M. Maier, M. Robertson, A. Vander Molen, and G. D. Westfall, Nucl. Instrum. Methods Phys. Res. A **337**, 619 (1994).
[5] Evaluated Nuclear Structure Data Files (Brookhaven National Laboratory, Upton, NY, 1997).
[6] D. E. Archer, E. A. Henry, and W. Younes, Bull. Am. Phys. Soc. **42**, 1687 (1997); (unpublished).
[7] G. Audi and A. H. Wapstra, Nucl. Phys. **A595**, 409 (1995).
[8] M. Blann, Phys. Rev. C **54**, 1341 (1996).
[9] W. Younes, in Proceedings of the First GEANIE Workshop, edited by D. Strottman and J. A. Becker, 1997 (unpublished).